NASA TECHNICAL NOTE

NASA TN D-6405

NASA TN D-6405

EXAMINATION OF BOUNDARY CONDITIONS FOR HEAT TRANSFER THROUGH A POROUS WALL

by Raymond S. Colladay and Francis S. Stepka

Lewis Research Center
Cleveland, Ohio 44135

NATIONAL AERONAUTICS AND SPACE ADMINISTRATION • WASHINGTON, D. C. • JULY 1971

1. Report No.	2. Government Accession No.	3. Recipient's Catalog No.
NASA TN D-6405		

4. Title and Subtitle
EXAMINATION OF BOUNDARY CONDITIONS FOR HEAT TRANSFER THROUGH A POROUS WALL

5. Report Date
July 1971

6. Performing Organization Code

7. Author(s)
Raymond S. Colladay and Francis S. Stepka

8. Performing Organization Report No.
E-6237

10. Work Unit No.
720-03

9. Performing Organization Name and Address
Lewis Research Center
National Aeronautics and Space Administration
Cleveland, Ohio 44135

11. Contract or Grant No.

13. Type of Report and Period Covered
Technical Note

12. Sponsoring Agency Name and Address
National Aeronautics and Space Administration
Washington, D.C. 20546

14. Sponsoring Agency Code

15. Supplementary Notes

16. Abstract

An analytical model describing the heat transfer through a porous wall is presented. It utilizes an experimental upstream wall heat-transfer coefficient as a boundary condition. An experiment was conducted to determine this coefficient for a surface simulating the surface of a typical full-coverage-film-cooled turbine blade, and the results are presented. The temperature rises of the coolant approaching normal to the upstream surface and through a porous wall are more reasonable with the proposed model than with previous models.

17. Key Words (Suggested by Author(s))
Heat transfer
Boundary condition
Porous

18. Distribution Statement
Unclassified - unlimited

19. Security Classif. (of this report)	20. Security Classif. (of this page)	21. No. of Pages	22. Price*
Unclassified	Unclassified	23	$3.00

*For sale by the National Technical Information Service, Springfield, Virginia 22151

EXAMINATION OF BOUNDARY CONDITIONS FOR HEAT TRANSFER THROUGH A POROUS WALL

by Raymond S. Colladay and Francis S. Stepka

Lewis Research Center

SUMMARY

An analytical model describing the heat transfer through a porous wall is presented. It utilizes an experimental upstream wall heat-transfer coefficient as a boundary condition. An experiment was conducted to determine this coefficient for a surface simulating the surface of a typical full-coverage-film-cooled turbine blade, and the results are presented.

The temperature rises of the coolant approaching normal to the upstream surface and through a porous wall are more reasonable with the proposed model than with previous models.

INTRODUCTION

An analytical model is developed in this report that can be used to predict the cooling air temperature rise and the metal temperatures through a porous wall. Previous analytical models for this purpose are presented in references 1 to 5. The most recent and comprehensive of the previous models (given in ref. 1), was utilized for the design of a full-coverage-film-cooled turbine blade at NASA. The results indicated that the rise in temperature of the cooling air as it approached normal to a porous turbine blade wall was greater than the rise through the wall even though the internal wall configuration was very effective from a heat-transfer standpoint. This apparent paradox led to the formulation of an alternative model which utilizes previously unavailable empirical data for the heat-transfer coefficient on the upstream surface of a porous wall.

This report (1) presents the proposed model, (2) presents the results of a preliminary experiment (conducted by the University of Minnesota under NASA contract) to determine the heat-transfer coefficients for flow normally approaching a typical perforated

wall configuration over a range of cooling air Reynolds numbers, and (3) compares the resulting model with that of reference 1.

ANALYSIS

In this section, a model for describing heat transfer from a porous wall is presented which utilizes, as a boundary condition, a Nusselt number correlation on the upstream face. Experimental data for this boundary condition were obtained by the University of Minnesota and are presented herein.

The model in reference 1 is singled out for comparison with the presently proposed model because it represents the most recent and comprehensive treatment of the subject and did make an attempt, with some success, to overcome some of the shortcomings of earlier investigations (refs. 2 to 5).

Heat-Transfer Models

Let model I refer to that presently proposed and model II to that of reference 1. The energy balance and resulting equations for coolant and porous matrix temperature for region I (see fig. 1) are the same for both models.

The heat-transfer process is described by assuming a one-dimensional model with constant properties where heat flowing by conduction through the wall in the negative x-direction is continuously transferred to the coolant in counterflow by convection. With the porous wall being composed of many small cooling passages within the matrix material, it is further assumed that conduction in the fluid in region I is negligible compared to that of the matrix.

Consider an element in a porous wall of area A normal to the x-direction as shown in figure 1. An energy balance on this element requires that the net heat conducted by the matrix into the element must be equal to the heat transferred by convection to the fluid; hence

$$k_e A \frac{d^2 T_w}{dx^2} \Delta x = h_m \Delta A_m (T_w - T_c)$$

where h_m is the internal matrix surface-to-coolant heat transfer coefficient, ΔA_m is the internal matrix surface area within the element, and k_e is the effective thermal conductivity of the porous wall. (All symbols are defined in appendix A.) Defining Z as the internal surface area per unit volume,

$$Z = \frac{\Delta A_m}{A \Delta_x}$$

leads to the following expression for the coolant temperature in region I:

$$T_c = T_w - \frac{k_e}{h_m Z} \frac{d^2 T_w}{dx^2} \tag{1}$$

For a homogeneous pore structure, Z is constant with x.

An energy balance on the coolant within the element in figure 1 gives

$$q'' = k_e \frac{d^2 T_w}{dx^2} \Delta x = G_c C_p \frac{dT_c}{dx} \Delta x$$

or

$$\frac{k_e}{G_c C_p} \frac{d^2 T_w}{dx^2} = \frac{dT_c}{dx} \tag{2}$$

Differentiating equation (1) with respect to x, neglecting entrance effects by assuming h_m constant, and substituting into equation (2) leads to the following equation for the temperature distribution in the matrix material:

$$\frac{d^3 T_w}{dx^3} + \frac{h_m Z}{G_c C_p} \frac{d^2 T_w}{dx^2} - \frac{h_m Z}{k_e} \frac{dT_w}{dx} = 0 \tag{3}$$

In dimensionless form, equations (1) and (3) become

$$\theta_c = \theta_w - \frac{1}{\lambda} \theta''_w \tag{4}$$

$$\theta'''_w + \beta \theta''_w - \lambda \theta'_w = 0 \tag{5}$$

where the prime denotes differentiation with respect to ξ, and

$$\theta_w = \frac{T_w - T_{c,\infty}}{T_{w,o} - T_{c,\infty}} \tag{6a}$$

$$\theta_c = \frac{T_c - T_{c,\infty}}{T_{w,o} - T_{c,\infty}} \tag{6b}$$

$$\xi = \frac{x}{L} \tag{6c}$$

$$\lambda = \frac{H_m L^2}{k_e} \tag{6d}$$

$$\beta = \frac{H_m L}{G_c C_p} \tag{6e}$$

where H_m is the internal volumetric heat-transfer coefficient equal to $h_m Z$.

The solution of equations (4) and (5) leads to the following expressions for the coolant and wall temperature profiles in region I:

$$\theta_w(\xi) = C_1 + C_2 e^{a_1 \xi} + C_3 e^{a_2 \xi} \tag{7}$$

$$\theta_c(\xi) = C_1 + C_2 \left(1 - \frac{a_1^2}{\lambda}\right) e^{a_1 \xi} + C_3 \left(1 - \frac{a_2^2}{\lambda}\right) e^{a_2 \xi} \tag{8}$$

where

$$a_1 = -\frac{1}{2}\left(\beta + \sqrt{\beta^2 + 4\lambda}\right) \tag{9a}$$

$$a_2 = -\frac{1}{2}\left(\beta - \sqrt{\beta^2 + 4\lambda}\right) \tag{9b}$$

Boundary Conditions

Model I. - Three boundary conditions are needed to evaluate the constants C_1, C_2, and C_3. These constants are in turn functions of λ and β, which are known parameters if the internal volumetric heat-transfer coefficient and effective thermal conductivity are known for the porous wall configuration.

The boundary conditions proposed are

$$\theta_w(1) = 1 \tag{11}$$

$$N\theta_w(0) = \theta'_w(0) \tag{12}$$

$$\theta_c(0) = \frac{\beta}{\lambda}\,\theta'_w(0) \tag{13}$$

where $N = h_i L/k_e$.

The first condition (eq. (11)) is that of a specified wall temperature $T_{w,o}$. The remaining two boundary conditions satisfy an energy balance at the interface at $x = 0$. It is assumed that the heat flux from the surface can be expressed as a product of a heat-transfer coefficient h_i and the temperature difference between the wall surface $T_{w,i}$ and the coolant supply $T_{c,\infty}$. Continuity of heat flux then gives

$$h_i(T_{w,i} - T_{c,\infty}) = k_e \left.\frac{dT_w}{dx}\right|_{x=0}$$

the dimensional form of equation (12). The heat-transfer coefficient must be obtained from an empirical correlation. This correlation should include the effect of coolant flow rate, geometrical hole array, hole spacing, hole diameter, etc.

Even though the flow in the vicinity of a hole is three-dimensional, on a large scale (compared to the hole diameter and spacing) where average temperatures in the $x = 0$ plane are desired, a one-dimensional analysis can be assumed.

The heat loss from the $x = 0$ face can also be expressed as

$$G_c C_p(T_{c,i} - T_{c,\infty}) = k_e \left.\frac{dT_w}{dx}\right|_{x=0}$$

which, when nondimensionalized, leads to equation (13). Note that the wall temperature $T_{w,i}$ and coolant temperature $T_{c,i}$ are a priori unknown.

The resulting expressions for the three constants in equations (7) and (8) are

$$C_1 = 0 \tag{14a}$$

$$C_2 = \frac{N - a_2}{(N - a_2)e^{a_1} - (N - a_1)e^{a_2}} \tag{14b}$$

$$C_3 = -\frac{N - a_1}{(N - a_2)e^{a_1} - (N - a_1)e^{a_2}} \tag{14c}$$

It is customary to evaluate the thermal performance of a porous wall in terms of its effectiveness η, where

$$\eta = \frac{T_{c,o} - T_{c,\infty}}{T_{w,o} - T_{c,\infty}} \tag{15}$$

Effectiveness is a measure of the efficiency of the porous wall as a mechanism for transferring heat to the coolant.

If the effectiveness is specified, then

$$\theta_c(1) = \eta \tag{16}$$

and the volumetric heat-transfer coefficient H_m can be calculated as a function of flow rate G_c by satisfying equation (16). Such a procedure, namely, that of satisfying a fourth boundary condition, is usually adopted in calculating the internal heat-transfer coefficient h_m. The internal matrix area per unit volume Z can often be found independently.

Regarding the coolant temperature, note that only the total temperature rise from $x = -\infty$ to $x = L$ is specified. How this total rise is distributed between regions I and II is a function of the model used to describe the heat-transfer process.

With the constants of integration thus evaluated, equations (7) and (8) may be used to evaluate all fluid and matrix temperatures in the wall. Only the outer wall temperature (or heat flux to the wall), coolant supply temperature, effectiveness (or volumetric heat transfer coefficient), and effective thermal conductivity are specified. If a heat flux boundary condition is given at $x = L$ with the wall temperature initially unknown, the boundary conditions for the model remain the same. However, to determine the dimensional temperature distributions, the exterior wall temperature must be calculated from the following overall energy balance equation:

$$q''(L) = G_c C_p \eta (T_{w,o} - T_{c,\infty})$$

If dimensionless temperatures are desired, only η (or H_m) and k_e are required.

Model II. - The boundary conditions for model II are presented in reference 1 and repeated in appendix B. Some of the symbols have been changed to be compatible with those of model I.

It should be noted that, in model II, the exponential coolant temperature profile for $x < 0$, given by equation (B3) occurs only if the flow in region II remains one-dimensional near the $x = 0$ face with no surface convection. However, an interface heat-transfer coefficient h_i for model II can be defined as follows:

$$q''_{x=0} = h_i\left[T_{c,\infty} - T_w(0)\right] = k_e \left.\frac{dT_w}{dx}\right|_{x=0} \tag{17}$$

or

$$\frac{k_e}{L}\theta'_w(0) = h_i\theta_w(0)$$

Hence,

$$h_i = \frac{k_e}{L}\frac{C_2a_1 + C_3a_2}{C_2 + C_3} \tag{18}$$

EXPERIMENTAL INVESTIGATION

Apparatus

The test section used to determine the heat-transfer coefficients for flow normally approaching a scaled-up model of a typical perforated wall of a turbine blade is shown schematically in figure 2. The surface of the wall at which the coefficient was determined consisted of a 0.025-mm- (0.001-in.-) thick sheet of stainless-steel shim stock. This sheet was cemeted to a base plate of 1.59-mm- (1/16-in.-) thick reinforced plastic, which in turn was bonded to a 7.62-cm- (3-in.-) thick layer of polyurethane foam insulation. This composite wall was a square 20.3 cm (8 in.) on a side, which had 36 holes, each 6.35 mm (1/4 in.) in diameter drilled through the wall. The holes were arranged in a square array with 5-diameter spacing. Cemeted to the edges of the wall were 1.27-cm- (1/2-in.-) thick plywood sheets to form the sides of a plenum chamber for the entering air.

The average heat-transfer coefficient at the surface of the perforated wall was obtained from the measured heat flux, the average surface temperatures, and the incoming air temperature.

The heat flux from the stainless-steel sheet (heater strip) was generated by electric current. This current was generated by a 6-volt battery. Leads from the battery were attached to copper bus bars that were soldered to opposite edges of the heater strip. The current flow was regulated by a variable resistor and determined by measuring the voltage drop across a shunt. The heat input to the heater strip was then determined from measured current flow and the resistance of the heater strip. The average temperature of the heater strip was obtained by arithmetically averaging the readings obtained from five iron-constantan thermocouples (shown in fig. 2) that were cememted to the back side of the heater strip. The thermocouples were electrically insulated from the heater strip by a thin layer of copper oxide. The inlet air temperature was measured by an iron-constantan thermocouple located in the center and about 20 hole diameters upstream of the test wall.

Ambient air was drawn to the test wall by means of a centrifugal blower downstream of the test section. The velocity approaching the wall was obtained from the measured flow, the wall area, and the inlet air density.

Procedure

The first set of data was obtained with the temperature difference between the heater strip and approaching coolant kept approximately constant while the air Reynolds number was changed. This was done to maintain constant fluid bouyant forces. In order to determine the sensitivity to these forces, another set of data was obtained wherein this temperature difference was varied at a constant Reynolds number.

RESULTS AND DISCUSSION

Experimentally obtained heat-transfer data for flow normally approaching a perforated wall are first discussed, and these data are then used in the discussion of the analytical models for heat transfer through porous walls.

Experimental Data

Nusselt number Nu_s for flow normally approaching a scaled-up model of a perforated wall surface of a typical full-coverage-film-cooled turbine blade is shown, in figure 3, to be linear on a log-log scale with flow Reynolds number Re_s. The characteristic dimension used in Nu_s and Re_s was the spacing between holes. The figure shows

that with no flow Nu_s due to natural convection was 5.4 and that with flow Nu_s increased to between 25 and 35 for Re_s of 500 and 2000, respectively. All the data used in this figure were obtained with a constant temperature difference of about 11 K between the wall and entering air.

The results of the test showing the effect of bouyant forces are shown in figure 4. For this test Re_s was maintained constant at 1650, and the temperature difference between the wall and the entering air was varied between 6 and 29 K. The results in the figure indicate that the effect on Nu_s was not large.

Only a limited number of variables were included in the empirical correlation for the heat-transfer coefficient presented herein. Additional experimental investigations will be required to include the effect of variables such as geometrical hole array, hole spacing, and hole diameter.

Analytical Models

For the purpose of comparing results from the two models, a typical full-coverage-film-cooled turbine blade wall composed of many small, closely spaced surface holes connected by a network of intricate torturous internal passages was chosen. The following conditions were assumed in the analysis:

Diameter of surface hole, d, mm	0.5
Hole spacing, S, diam	5
Effective thermal conductivity, k_e, J/(sec)(m)(K)	5.2
Wall thickness, L, mm	0.5
Effectiveness, η	0.7

Frequently, the effectiveness of a porous wall is assumed to be unity. However, for turbine blade applications where wall thickness is small and the amount of area in contact with the coolant is limited η is usually less than 1 (refs. 1 and 2). In reference 6, values of η from 0.6 to 0.8 were assumed as typical of many blade wall configurations. Over a range of coolant flow rates of practical interest, it has been observed that typical full-coverage-film-cooled walls exhibit effectiveness values which do not vary significantly with flow rate. For this study a constant value of 0.7 was assumed.

Internal heat-transfer coefficient. - There exists a unique value of internal volumetric heat-transfer coefficient H_m which satisfies equation (16) for a given mass velocity at a specified effectiveness. For each model, the H_m distribution as a function of G_c, which satisfies an effectiveness value of 0.7, is determined and presented in figure 5. The magnitude of the internal coefficient is significantly greater for model I than for model II, and the slope is less. The ratio of the slopes for model I to II is 0.74. At a G_c value of 0.35 g/(sec)(cm^2), representative of that expected in many turbine applica-

tions, the H_m ratio (and consequently the h_m ratio) is 1.93. The specific value of the slope is a function of the variation of η with G_c. The slope is greater for a constant effectiveness than it would be if η decreased with increasing G_c.

Back-face heat-transfer coefficient. - The h_i distribution used in the boundary condition given by equation (13) for model I was obtained from the experimental results given in figure 3 with the appropriate hole diameter and spacing.

Although a back-face heat-transfer coefficient is not required for model II, it is an implicit result of the model and can be calculated by equation (18). The resulting h_i distribution, given as a function of G_c, is shown in figure 6 along with the experimental value used in model I. The coefficient calculated from model II is considerably greater than would be expected on the basis of the experimental results. For example, at a G_c value of 0.35 g/(sec)(cm^2), the h_i ratio for model II to I is 4.6.

Actually, model II implies no convection on the $x = 0$ surface. However, the coefficient h_i is defined by equation (17) to give the convective equivalent of the back-face heat flux that occurs only by conduction upstream within the coolant.

Temperature profiles. - For a mass velocity of 0.35 g/(sec)(cm^2), the dimensionless temperature distributions of the matrix and coolant for each model are given in figure 7. The difference in the coolant temperature distribution for the two models is consistent with the relative magnitudes of the heat-transfer coefficients h_i and H_m between the models.

The treatment of the $x = 0$ boundary or interface conditions has a much greater effect on the coolant temperature than on the wall temperature. The assumption in model II using the asymptotic value for $\theta''_w(0)/\theta'_w(0)$ (eq. (B9)) strongly affects the heat flux at $x = 0$. However, since the wall temperature gradiant at $x = 0$ must be less than at $x = L$, the effect of this assumption on the wall temperature is small. It should be noted that, though model II forces the asymptotic relation at $x = 0$ for all G_c, model I reduces to the same case if the coolant flow rate is large.

The coolant temperature distribution for model II predicts that 72 percent of the total temperature rise occurs upstream of the back face, as compared to 17.2 percent for model I. It was this distribution between the coolant temperature rise approaching the wall and through the wall that caused the initial concern when model II was applied to a similar cooling situation.

Often the internal heat-transfer performance of a wall configuration alone, exclusive of the upstream ($x < 0$) region, is desired. In that case, a useful parameter is the wall internal effectiveness defined as

$$\eta_w = \frac{T_{c,o} - T_{c,i}}{T_{w,o} - T_{c,i}}$$

When related to the overall wall effectiveness η, this equation becomes

$$\eta_w = \frac{\eta - \theta_c(0)}{1 - \theta_c(0)}$$

In the present example, model II predicts an η_w value of 0.4, while model I gives 0.66.

CONCLUDING REMARKS

The experimental heat-transfer performance on the upstream surface of a perforated wall with normally approaching flow was obtained. This perforated surface simulated the surface of a typical full-coverage-film-cooled turbine blade.

An analytical model describing the heat transfer through a porous wall was proposed. It utilizes experimental data for the upstream heat-transfer coefficient as a boundary condition. As a result, reasonable temperature rises of the coolant approaching normal to the upstream surface and through the porous wall were obtained.

Because of the limited number of variables included in the empirical correlation for the upstream surface heat-transfer coefficient presented herein, it would be desirable if the experimental study could be extended to include the effect of variables, such as geometrical hole array, hole spacing, and hole diameter.

Lewis Research Center,
National Aeronautics and Space Administration,
Cleveland, Ohio, April 7, 1971,
720-03.

APPENDIX A

SYMBOLS

a_1, a_2	parameters defined by eqs. (9a) and (9b)
C_p	specific heat
C_1, C_2, C_3	constants of integration
d	hole diameter
G_c	surface averaged coolant mass velocity, ρu
H_m	porous matrix internal volumetric heat-transfer coefficient, $h_m Z$
h_i	heat-transfer coefficient for $x = 0$ face
h_m	heat-transfer coefficient for inside porous matrix
k	thermal conductivity
L	wall thickness
N	dimensionless heat-transfer coefficient parameter, $h_i L/k_e$
Nu	Nusselt number
q''	heat flux
Re	Reynolds number
S	distance between holes
T	temperature
u	approach velocity
x	spacial coordinate normal to wall
Z	porous matrix internal surface area per unit volume
α	parameter defined by eq. (B2)
β	parameter defined by eq. (6e)
η	overall effectiveness, $\frac{T_{c,o} - T_{c,\infty}}{T_{w,o} - T_{c,\infty}}$
η_w	wall internal effectiveness, $\frac{T_{c,o} - T_{c,i}}{T_{w,o} - T_{c,i}}$
θ	dimensionless temperature, $\frac{T - T_{c,\infty}}{T_{w,o} - T_{c,\infty}}$

λ	parameter defined by eq. (6d)
ν	kinematic viscosity
ξ	dimensionless x variable, x/L
ρ	density

Subscripts:

c	coolant
e	effective wall
i	location at x = 0
o	location at x = L
s	hole spacing
w	wall
∞	location at $x = -\infty$
II	coolant in region II

APPENDIX B

BOUNDARY CONDITIONS FOR MODEL II

The model of reference 1 (designated model II) attempts to describe analytically the behavior of the coolant in region II (see fig. 1) which, with accompanying continuity conditions at the interface between the two regions, allows a complete closed-form analytical solution to the problem without explicitly specifying any heat flux condition at the $x = 0$ face.

An energy balance on a fluid element in region II yields the following convection-conduction counterflow differential equation:

$$k_c \frac{d^2T_{II}}{dx^2} = G_c C_p \frac{dT_{II}}{dx} \tag{B1}$$

which in dimensionless form becomes

$$\theta''_{II} - \alpha \theta'_{II} = 0 \tag{B2}$$

where

$$\alpha = \frac{G_c C_p L}{k_c}$$

$$\theta_{II} = \frac{T_{II}(\xi) - T_{c,\infty}}{T_{w,o} - T_{c,\infty}}$$

Integrating equation (B2) and repeating equations (7) and (8) give for model II

$$\theta_{II}(\xi) = C_4 + C_5 e^{\alpha \xi} \tag{B3}$$

$$\theta_w(\xi) = C_1 + C_2 e^{a_1 \xi} + C_3 e^{a_2 \xi} \tag{7}$$

$$\theta_c(\xi) = C_1 + C_2\left(1 - \frac{a_1^2}{\lambda}\right)e^{a_1\xi} + C_3\left(1 - \frac{a_2^2}{\lambda}\right)e^{a_2\xi} \tag{8}$$

Five boundary conditions are needed to solve for the constants of integration, and there is an added sixth condition if the volumetric heat-transfer coefficient is not specified. The five boundary conditions are

$$\theta_w(1) = 1 \tag{11}$$

$$\theta_{II}(-\infty) = 0 \tag{B5}$$

$$\theta_{II}(0) = \theta_c(0) \tag{B6}$$

$$\theta'_w(0) = \frac{\lambda}{\alpha\beta}\,\theta'_{II}(0) \tag{B7}$$

$$\theta'_c(0) = \frac{\lambda}{\alpha\beta}\,\theta'_{II}(0) \tag{B8}$$

The first two boundary conditions are for specified outer wall temperature and coolant supply temperature, respectively. Equations (B6) and (B7) are $x = 0$ interface conditions requiring continuity of coolant temperature and heat flux, respectively. In equation (B7), note that $k_c/k_e = \lambda/\alpha\beta$.

The interface condition in equation (B8) requires more explanation. Because conduction through the coolant in region I was neglected, a discontinuity in the slope of the coolant temperature at $x = 0$ will result. A relation between these two slopes ($\theta'_c(0)$ and $\theta'_{II}(0)$) can be found by combining equations (2), (B1), and (B7):

$$\left.\frac{dT_c}{dx}\right|_{x=0} = \frac{k_c}{G_c C_p}\left(\frac{\dfrac{d^2T_w}{dx^2}}{\dfrac{dT_w}{dx}}\right)_{x=0}\left.\frac{dT_{II}}{dx}\right|_{x=0} \tag{B9}$$

It is then assumed that the ratio of second to first derivatives of the wall temperature at $x = 0$ can be obtained from the limiting case where the coolant and matrix temperatures

in region I are everywhere equal, that is, $h_i = \infty$ and $\eta = 1$. For this classical case (see ref. 3), equation (2) reduces to

$$\frac{d^2T}{dx^2} - \frac{G_c C_p}{k_e} \frac{dT}{dx} = 0$$

where $T_w = T_c = T$, and the boundary conditions become

$$k_e \left.\frac{dT}{dx}\right|_{x=0} = G_c C_p \left[T(0) - T_{c,\infty}\right]$$

$$T(L) = T_w$$

The solution in dimensionless form is readily obtained as

$$\theta(\xi) = e^{\frac{\lambda}{\beta}(\xi-1)} \tag{B10}$$

and

$$\frac{\theta''(0)}{\theta'(0)} = \frac{\lambda}{\beta} = \frac{\theta''_w(0)}{\theta'_w(0)} \tag{B11}$$

Substituting equation (B11) into (B9) yields the interface condition given in equation (B8).

The resulting expressions for the five constants of integration are

$$C_1 = 0$$

$$C_2 = \frac{b_2(1 - b_2)}{b_2(1 - b_2)e^{a_1} - b_1(1 - b_1)e^{a_2}} \tag{B12}$$

$$C_3 = -\frac{b_1(1 - b_1)}{b_2(1 - b_2)e^{a_1} - b_1(1 - b_1)e^{a_2}}$$

$$C_4 = 0$$

$$C_5 = b_1 C_2 + b_2 C_3$$

where

$$b_1 = \frac{\beta a_1}{\lambda}$$

$$b_2 = \frac{\beta a_2}{\lambda}$$

The constants C_2, C_3, and C_5 are functions of β and λ, which are in turn a function of H_m. However, the local matrix and coolant temperatures given by equations (7), (8), and (B3) can be evaluated without explicitly specifying H_m if the effectiveness condition (eq. (16)) is satisfied.

REFERENCES

1. Nealy, David A.; and Anderson, R. Daryel: Heat Transfer Characteristics of Laminated Porous Materials. Rep. EDR-5856, General Motors Corp. (AFAPL-TR-68-98, AD-391895), Aug. 1968.

2. Bernicker, Richard P.: An Investigation of Porous Wall Cooling. Paper 60-WA-233, ASME, 1960.

3. Schneider, Paul J.: Conduction Heat Transfer. Addison-Wesley Pub. Co., 1955, pp. 218-226.

4. Schneider, P. J.; and Brogan, J. J.: Temperature Response of a Transpiration-Cooled Plate. ARS J., vol. 32, no. 2, Feb. 1962, pp. 233-236.

5. Weinbaum, Sidney; and Wheeler, H. L., Jr.: Heat Transfer in Sweat-Cooled Porous Metals. J. Appl. Phys., vol. 20, no. 1, Jan. 1949, pp. 113-122.

6. Esgar, Jack B.; Colladay, Raymond S.; and Kaufman, Albert: An Analysis of the Capabilities and Limitations of Turbine Air Cooling Methods. NASA TN D-5992, 1970.

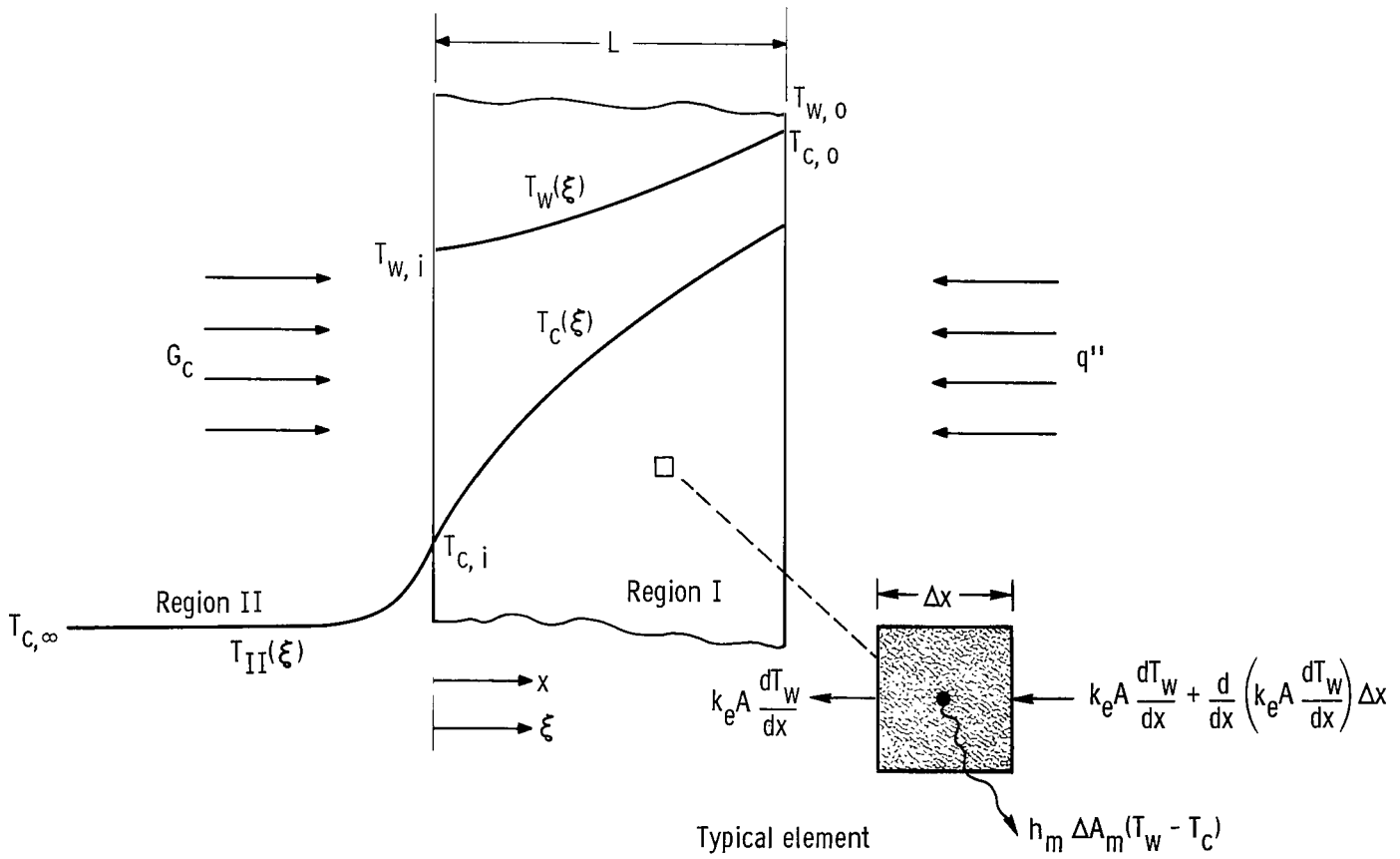

Figure 1. - Porous wall temperature profile model.

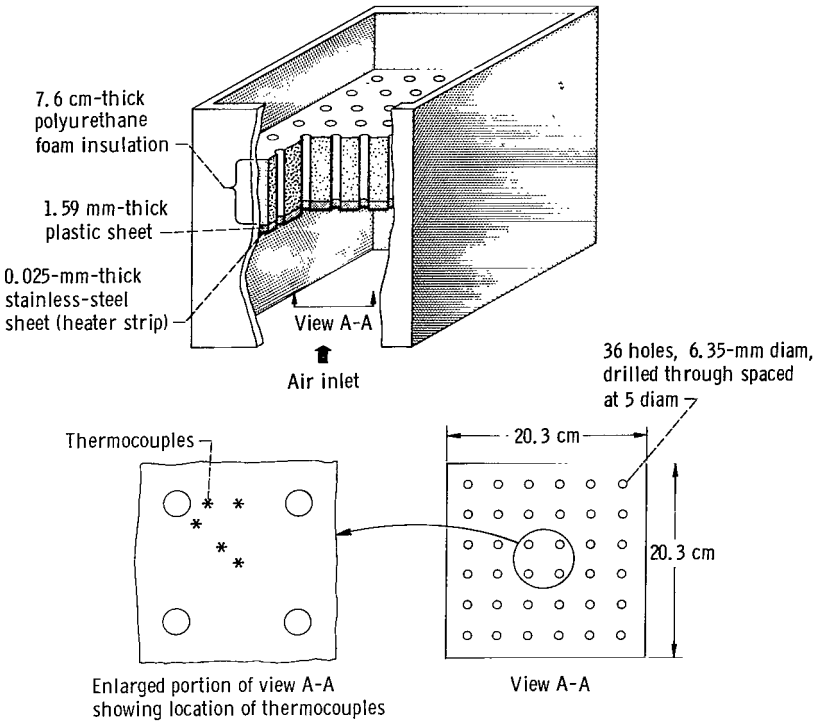

Figure 2. - Schematic of test section used to determine heat-transfer coefficients for flow normally approaching a perforated wall.

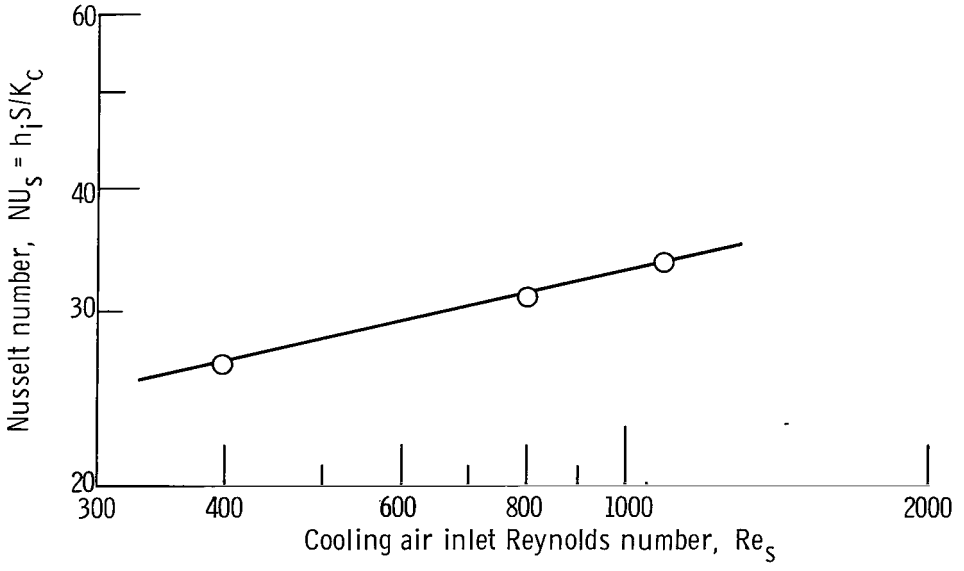

Figure 3. - Nusselt number for flow normally approaching perforated wall. Temperature difference between wall and coolant, ≈11 K); at Reynolds number of 0, Nusselt number is 5.4.